

## New TM5-4DVAR inverse modelling system to estimate global and European CH<sub>4</sub> sources

Peter Bergamaschi<sup>1</sup>, Jan Fokke Meirink<sup>2</sup>, Maarten Krol<sup>2,3</sup>, and Maria Gabriella Villani<sup>1</sup>

[1] European Commission DG Joint Research Centre, Institute for Environment and Sustainability, Ispra, Italy

[2] Institute for Marine and Atmospheric Research Utrecht, University of Utrecht, The Netherlands

[3] Wageningen University and Research Centre, Wageningen, The Netherlands

### Introduction

A new, 4-dimensional variational (4DVAR) inverse modelling system has been developed for inverse modelling of atmospheric methane. The main advantage of the new system is that it allows optimizing emissions of individual model grid cells. At the same time very large sets of observational data can be used (e.g. high-frequency in situ measurements or satellite data). In contrast, the previously widely used synthesis inversions were restricted to the optimization of emissions of larger, pre-defined regions (e.g. continents, or countries), but could not further optimize spatial emission distributions within these pre-defined regions. Therefore, these approaches were prone to the so-called aggregation error [Kaminski *et al.*, 2001].

### 4DVAR technique

4DVAR techniques are widely used in numerical weather prediction in order to optimize the initial state of the atmosphere. For application to inverse modelling, we extend the state vector, including the (1) initial 3D atmospheric mixing ratios, (2) monthly emissions per grid cell (and optionally also per emission category), and (3) further parameters as e.g. bias corrections for satellite data.

The cost function:

$$J(\vec{x}) = \frac{1}{2}(\vec{x} - \vec{x}_B)^T \mathbf{B}^{-1}(\vec{x} - \vec{x}_B) + \frac{1}{2} \sum_{i=1}^n (\vec{y}_{OBS,i} - \vec{H}_i(\vec{x}))^T \mathbf{R}_i^{-1} (\vec{y}_{OBS,i} - \vec{H}_i(\vec{x}))$$

(with  $\vec{x}$ : state vector;  $\vec{x}_B$ : *a priori* estimate of  $\vec{x}$ ;  $\mathbf{B}$  background error covariance matrix;  $\vec{y}_{OBS}$ : observations;  $\vec{H}(\vec{x})$  model simulations of observations;  $\mathbf{R}$  observations error covariance matrix;  $i$  index of assimilation time window)

is minimized iteratively, by evaluating its gradient:

$$\vec{\nabla} J(\vec{x}) = \mathbf{B}^{-1}(\vec{x} - \vec{x}_B) - \sum_{i=1}^n \mathbf{M}_i^T \cdots \mathbf{M}_{i-1}^T \mathbf{M}_i^T \mathbf{H}_i^T \mathbf{R}_i^{-1} (\vec{y}_{OBS,i} - \vec{H}_i(\vec{x}))$$

(with  $\mathbf{M}$ : atmospheric transport model;  $\mathbf{M}^T$ : adjoint of  $\mathbf{M}$ ;  $\mathbf{H}$  observation operator) and applying the ECMWF conjugate gradient minimization algorithm [Fisher and Courtier, 1995]. We apply the atmospheric transport TM5 [Krol *et al.*, 2005], and developed its adjoint model for this purpose. Figure 1 shows the iterative

minimization for a 1-year global 4DVAR inversion, illustrating the very rapid decrease of the gradient norm.

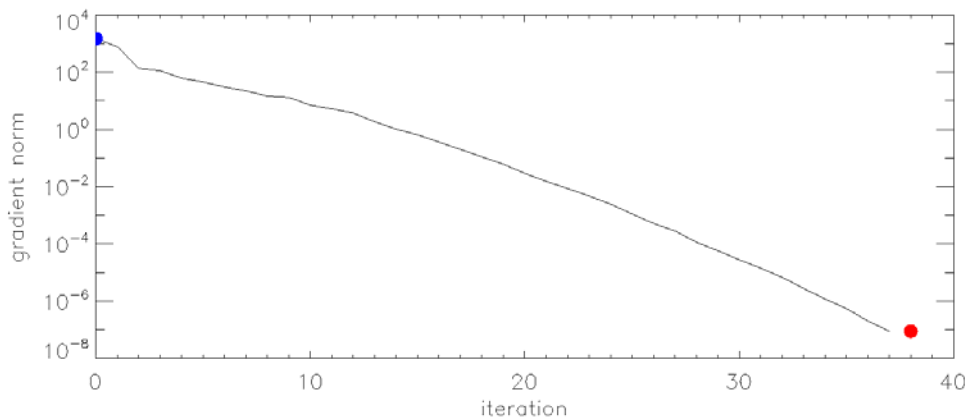


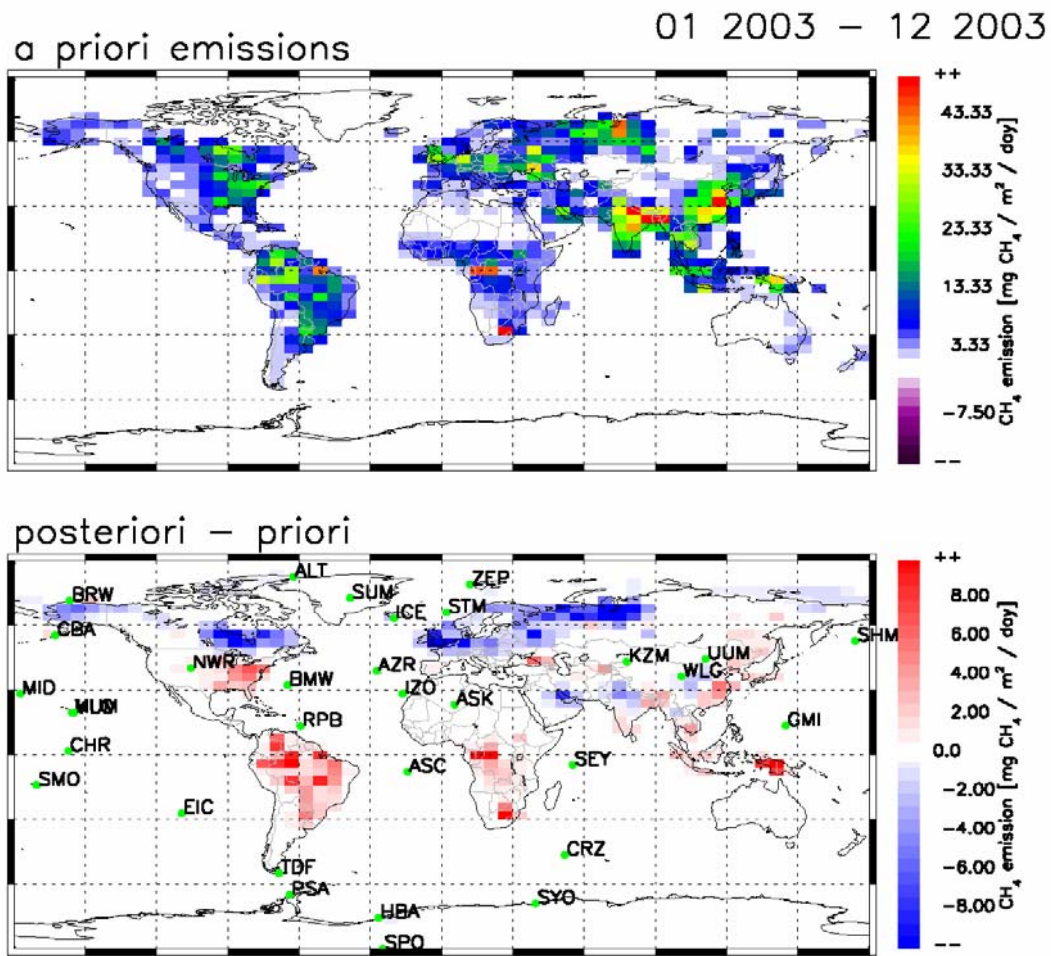
**Figure 1:** Reduction of gradient norm by iterative 4DVAR minimization using the ECMWF conjugate gradient algorithm.

### First global 4DVAR inversions and comparison with synthesis inversion

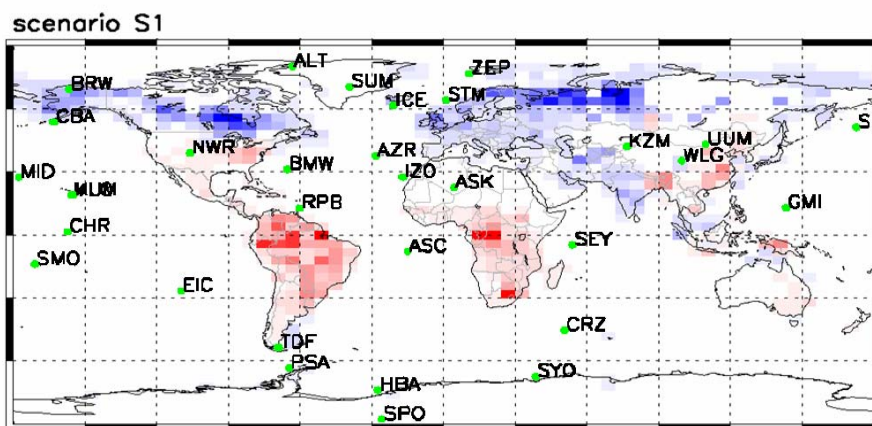
Figure 2 shows an example of a global 4DVAR inversion, using *a priori* emissions from 11 different source categories. We assumed constant uncertainties of monthly emissions per grid cell, ranging between 20 and 80% for the different source categories. Furthermore, a spatial decorrelation length of 500 km was assumed. As observational data we used the CH<sub>4</sub> surface measurements from the NOAA network ([Dlugokencky *et al.*, 1994], background sites only).

The 4DVAR inversion leads to some redistribution between NH and SH sources, and, as large scale regional features, increased emissions over the Amazon and tropical Africa, and decreased emissions over Canada and Siberia.

We compare these results with results from a recent synthesis inversion (Figure 3), for which the same *a priori* emission inventories and the same observational data were used, and for which 7 big global regions were defined (this synthesis inversion is described in detail in [Bergamaschi *et al.*, 2007]). Obviously, despite the limitations of the synthesis inversion, the agreement between both approaches is surprisingly good: This is attributed to the fact that the synthesis inversion with the 11 source categories already provides relatively high flexibility. Furthermore, the applied background observations do not provide strong constraints on emissions of individual model grid cells, but rather on larger scale emissions.



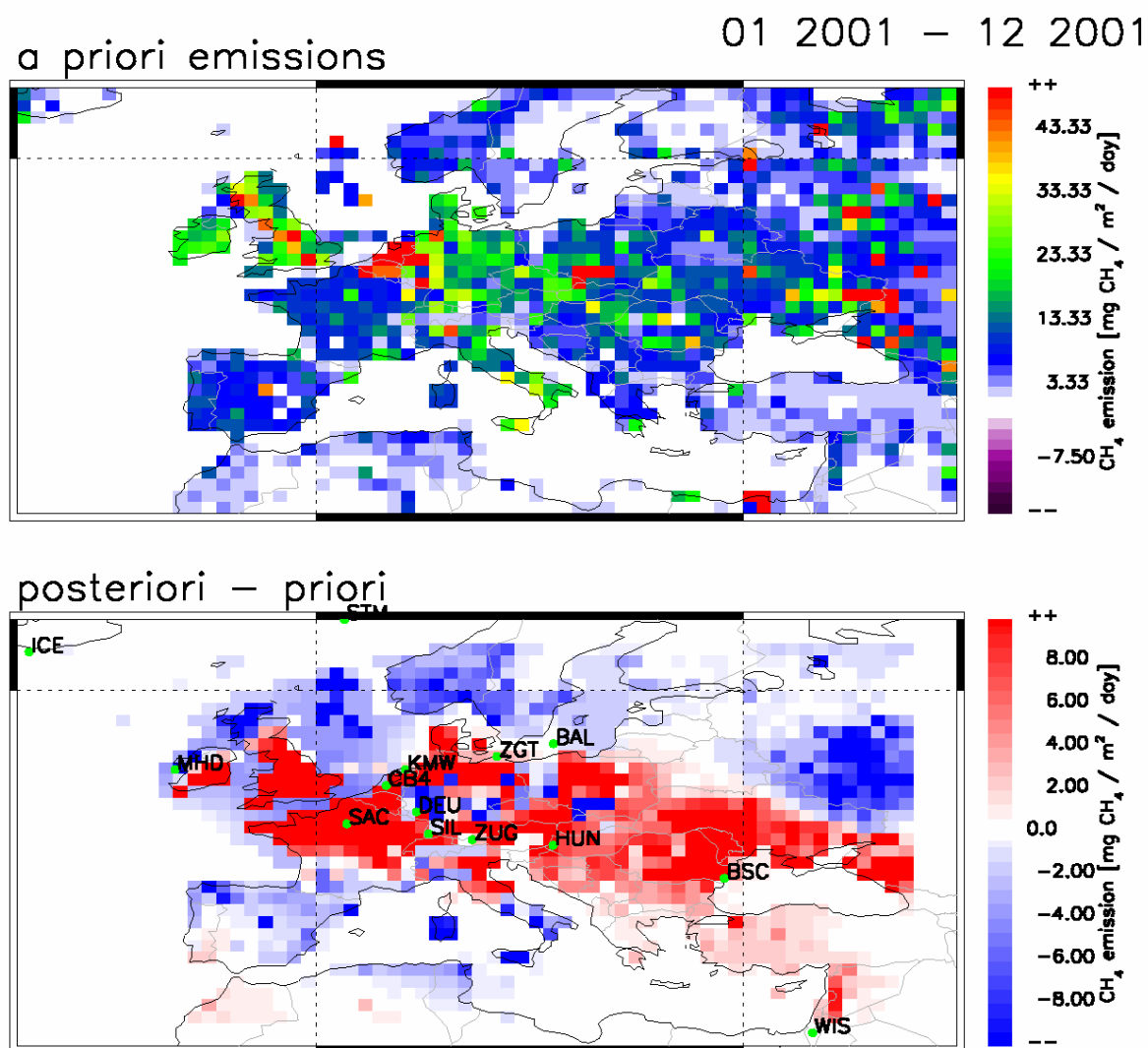
**Figure 2:** Global 4DVAR inversion for year 2003 using surface background observations from the NOAA network. Upper panel: *a priori* emissions; lower panel: Inversion increment (i.e. *a posteriori* - *a priori* emissions).



**Figure 3:** Inversion increment for synthesis inversion [Bergamaschi et al., 2007].

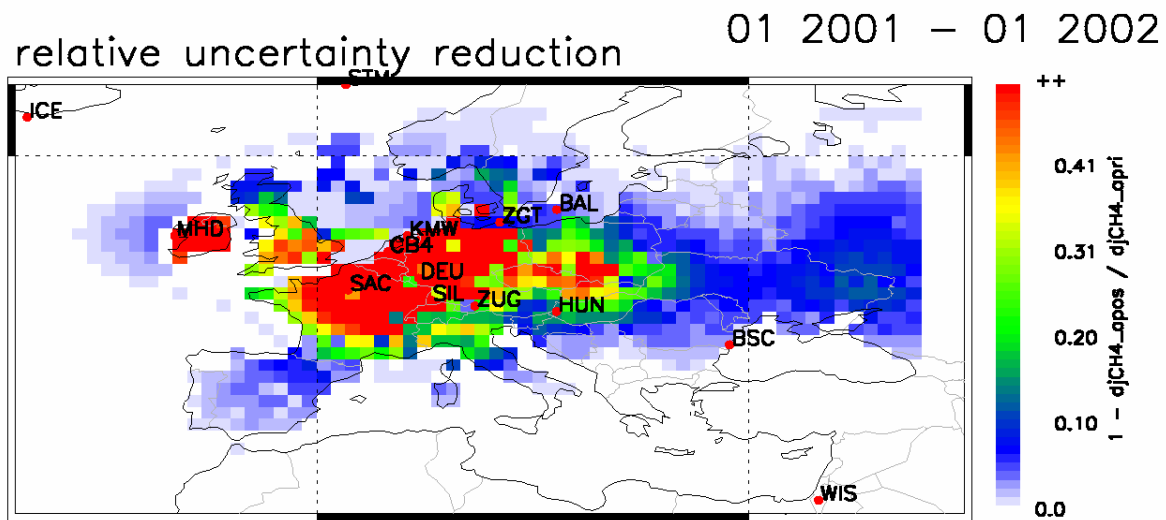
## First European TM5-4DVAR inversions

Figure 4 shows a coupled global - European inversion, applying the  $1^\circ \times 1^\circ$  zooming over the European domain. Observational data include a number of high-frequency observations over Europe (and are identical to those used in a country-based synthesis inversion [Bergamaschi et al., 2005]; however we use here different *a priori* emission inventories for the 4DVAR inversion). The first results for a series of 4DVAR scenarios yield *a posteriori* total emissions for the EU-15 countries close to those derived from the synthesis inversion (20-23 Tg  $\text{CH}_4/\text{yr}$  derived in the synthesis inversion for scenarios S1-S9 [Bergamaschi et al., 2005]). The influence of the *a priori* emissions and further parameters of the 4DVAR system are currently further investigated.



**Figure 4:** Coupled global-European 4DVAR inversion for year 2001 using high-frequency observations from several European monitoring stations (complemented by European and global flask measurements). Upper panel: *a priori* emissions; lower panel: Inversion increment (i.e. *a posteriori* - *a priori* emissions).

Figure 5 shows the achieved uncertainty reduction in the 4DVAR inversion (approximation based on leading eigenvectors). The figure illustrates the significant uncertainty reduction in particular close to high-frequency observations.



**Figure 5:** Uncertainty reduction achieved by 4DVAR inversion.

## Conclusions

- The new 4DVAR inverse modelling system allows flexible optimization of complex systems with very large numbers of parameters (emissions from individual model grid cells) and very large numbers of observations (both in the order of  $10^4 - 10^6$ ).
- First 4DVAR results show high consistency with previous synthesis inversions (both on global and European scale). The much higher flexibility of the 4DVAR system becomes apparent when using continental high-frequency surface observations (or satellite data), minimizing the 'aggregation-error'.
- The first preliminary results of the European 4DVAR inversion yield total  $\text{CH}_4$  emissions from EU-15 countries close to previous synthesis inversions [Bergamaschi et al., 2005].

## Acknowledgments

We are grateful to the NOAA, AGAGE, and GAW networks for the provision of their observational data. Furthermore, we thank A. Vermeulen, M. Ramonet, and F. Meinhardt for delivery of high-frequency measurements at various European monitoring stations.

## References

Bergamaschi, P., C. Frankenberg, J.F. Meirink, M. Krol, F. Dentener, T. Wagner, U. Platt, J.O. Kaplan, S. Körner, M. Heimann, E.J. Dlugokencky, and A. Goede, Satellite cartography of atmospheric methane from SCIAMACHY onboard ENVISAT: (II)

- Evaluation based on inverse model simulations, *J. Geophys. Res.*, 112, D02304, doi:10.1029/2006JD007268, 2007.
- Bergamaschi, P., M. Krol, F. Dentener, A. Vermeulen, F. Meinhardt, R. Graul, M. Ramonet, W. Peters, and E.J. Dlugokencky, Inverse modelling of national and European CH<sub>4</sub> emissions using the atmospheric zoom model TM5, *Atmos. Chem. Phys.*, 5, 2431-2460, 2005.
- Dlugokencky, E. J., L. P. Steele, P. M. Lang, and K. A. Masarie, The growth rate and distribution of atmospheric methane, *J. Geophys. Res.*, 99, 17,021– 17,043, 1994.
- Fisher, M. and P. Courtier, Estimating the covariance matrices of analysis and forecast error in variational data assimilation. Technical Memorandum 220, ECMWF, Reading, U.K., 1995.
- Kaminski, T., P. J. Rayner, M. Heimann, and I. G. Enting, On aggregation errors in atmospheric transport inversions. *J. Geophys. Res.*, 106, 4703–4715, 2001.
- Krol, M.C., S. Houweling, B. Bregman, M. van den Broek, A. Segers, P. van Velthoven, W. Peters, F. Dentener, and P. Bergamaschi, The two-way nested global chemistry-transport zoom model TM5: algorithm and applications, *Atmos. Chem. Phys.*, 5, 417-432, 2005.
- Meirink J.F., Bergamaschi P., and Krol M.: Four-dimensional variational data assimilation for inverse modelling of methane emissions, paper in preparation, 2007,
- Meirink, J.F., H.J. Eskes, and A.P.H. Goede, Sensitivity analysis of methane emissions derived from SCIAMACHY observations through inverse modelling, *Atmos. Chem. Phys.*, 6, 1275-1292, 2006.